Polymer 52 (2011) 1944–1953

Contents lists available at ScienceDirect

Polymer

journal homepage: www.elsevier.com/locate/polymer

Kinetics of free radical polymerization probed by dielectric relaxation spectroscopy under high conductivity conditions

M.T. Viciosa [a,*], M. Dionísio [b], J.L. Gómez Ribelles [c,d,e]

[a] CQFM – Centro de Química-Física Molecular and IN – Instituto of Nanoscience and Nanotechnology, Instituto Superior Técnico, Universidade Técnica de Lisboa, Avenida Rovisco Pais, 1049-001 Lisbon, Portugal
[b] REQUIMTE, Departamento de Química, Faculdade de Ciências e Tecnologia da, Universidade Nova de Lisboa, 2829-516 Caparica, Portugal
[c] Centro de Biomateriales e Ingeniería Tisular, Universidad Politécnica de Valencia, Camino de Vera s/n, E-46022 Valencia, Spain
[d] Centro de Investigación Príncipe Felipe, Avda. Autopista del Saler 16, 46013 Valencia, Spain
[e] CIBER en Bioingeniería, Biomateriales y Nanomedicina, Valencia, Spain

ARTICLE INFO

Article history:
Received 16 December 2010
Received in revised form
15 February 2011
Accepted 2 March 2011
Available online 9 March 2011

Keywords:
Electric modulus
Free radical polymerization
TrEGDMA

ABSTRACT

Polymerization kinetics of tri-ethylene glycol dimethacrylate (TrEGDMA)/2,2-azobis-isobutyronitrile (AIBN) mixtures (0.1% w.t.) at different temperatures was investigated by using dielectric relaxation spectroscopy. The dielectric spectra at the polymerization temperatures studied are dominated by high conductivity leading us to employ the electric modulus representation in order to extract information about the evolution of the system during isothermal reaction. An intense peak appears in the imaginary component of the complex dielectric modulus which is related to conductivity. The variation of the strength of this peak and of its relaxation time with the polymerization time allows us to determine the polymerization degree evolution and the moment in which vitrification is attained, which can be compared with results obtained by temperature modulated DSC in a previous work (Viciosa MT, Hoyo JQ, Dionísio M, Gómez Ribelles JL. Journal of Thermal Analysis and Calorimetry 2007; 90:407–414).

The study was completed with a detailed analysis of conductivity carried out in the unreacted system using both dielectric modulus and conductivity representations.

1. Introduction

The study of the kinetics of polymerization reactions using techniques such as DSC or IR have some limitations in the case of fast kinetics due to the large times of stabilization and/or measuring times. Such fast reactions take place for instance in the case of free radical polymerization using photosensible initiators or redox pairs. These situations are met for instance in biomedical applications, in the case of dental materials or bone cements, in both cases polymerization takes place in situ and there is much interest in characterizing the dependence of the reaction kinetics (and related properties such as the rate of heat liberation to the host tissue or the material contraction) and initiator content, temperature, light sources etc.

In these cases dielectric relaxation can be very useful since it allows, particularly when measuring at high frequency, taking a great number of data points in short times and also because it is possible to design dielectric cells simulating the shape and volume of the real situations.

Dielectric relaxation spectroscopy, DRS, has been extensively used in the study of epoxy curing reactions [1–5], and in the polymerization of linear chains as well. In that studies the probe for the curing kinetics was the shift of the main dielectric relaxation, of dipolar origin. The glass transition temperature of the system consisting in the mixture of the growing polymer network or growing polymer chains and the unreacted monomer strongly depends on composition, *i.e.* low-molecular weight monomer concentration that acts as plasticizer of the polymer segments. As a consequence, as polymerization progresses glass transition temperature increases and the main relaxation peak shifts toward longer times or lower frequencies when measured in real time at constant temperature. In the case of free radical polymerization the situation is much different since the presence of free radical ions highly increases dc conductivity. The high conductivity of the system even for high conversion degrees prevents the characterization of the dipolar relaxation. But actually dc conductivity is a good probe to monitor polymerization kinetics since it depends exponentially on the difference between the measuring temperature and the glass transition temperature of the polymer system.

* Corresponding author. Fax: +351 218464455.
E-mail address: teresaviciosa@ist.utl.pt (M.T. Viciosa).

0032-3861/$ – see front matter © 2011 Elsevier Ltd. All rights reserved.
doi:10.1016/j.polymer.2011.03.006

1.1. Dielectric modulus formalism

Dielectric modulus is the dielectric analoganalog of the elastic modulus [6]. Obviously it cannot be directly measured since there is no dielectric analogue to the stress relaxation viscoelastic experiments. Nevertheless, within the linear viscoelastic or dielectric range, dielectric modulus can be calculated from permittivity as elastic modulus can be calculated from compliance. In the case of sinusoidal excitation of the sample the complex dielectric modulus

$$M^* = M' + iM'' \tag{1}$$

and complex dielectric permittivity

$$\varepsilon^* = \varepsilon' + i\varepsilon'' \tag{2}$$

are related through [7] [8],

$$M'' = \frac{\varepsilon''}{\varepsilon'^2 + \varepsilon''^2} \tag{3}$$

The contribution of dc conductivity to the complex dielectric permittivity is characterized by

$$\varepsilon'' = \frac{1}{\rho\omega\varepsilon_0} \tag{4}$$

Where ρ is the resistivity of the material $\rho = 1/\sigma_0$ while ε' is frequency independent.

If Equation 4 is introduced in Equation 3 one obtain

$$M'' = \frac{1/\rho\omega\varepsilon_0}{1/(\rho\omega\varepsilon_0)^2 + \varepsilon'^2} = \frac{(\rho\varepsilon'\varepsilon_0)\omega 1/\varepsilon'}{1 + (\rho\varepsilon'\varepsilon_0)^2\omega^2} \tag{5}$$

The form of Equation 5 is identical to that found for a single relaxation time process

$$M'' = \Delta M\frac{\omega\tau}{1 + \omega^2\tau^2} \tag{6}$$

where $\tau = \rho\varepsilon'\varepsilon_0$. Note that the product $\rho\varepsilon_0$ has time dimensions.

Thus, the evolution of the dc conductivity of the system during polymerization can be analyzed in the dielectric modulus formalism as an evolution of $\tau = \rho\varepsilon'\varepsilon_0$ with the dimensions of a relaxation time. As the polymerization progresses, conductivity decreases due to the decrease of the free charge carriers number and mobility. The increase of the viscosity of the system produces an increase in τ. The advantage of the manipulation of the permittivity results in this way is that the relaxation time $\tau = \rho\varepsilon'\varepsilon_0$ is determined as the reciprocal of the frequency at which M″ goes through its maximum.

Note that the use of the modulus formalism is being carried out principally in a temperature region where no relaxation process takes place as confirmed by the frequency independence of ε′, being just a way to present the results that allow an easy following up of the polymerization process.

In this work we show how real time isothermal dielectric measurements allow characterizing polymerization kinetics. To do that free radical polymerization of tri-ethylene glycol dimethacrylate, TrEGDMA, was performed isothermally in a broad temperature range using a thermal initiator allowing to compare the results obtained with those of temperature modulated differential scanning calorimetry previously published [9].

2. Experimental

The tri-ethylene glycol dimethacrylate monomer with the formula shown in Fig. 1, with $n = 3$ and Mw = 286.36 was supplied by Fluka, cat. nbr. 90412. The monomer was previously passed through a disposable inhibitor remover column from Aldrich, ref. 306312-1EA, in order to eliminate the hydroquinone stabilizer. The polymerization initiator was 2,2-azobis-isobutyronitrile (AIBN) from Aldrich, cat. nbr. 11630. Only one solution was prepared in air by dissolving 0.1% w.t. of AIBN in TrEGDMA and it was used in all the samples polymerized.

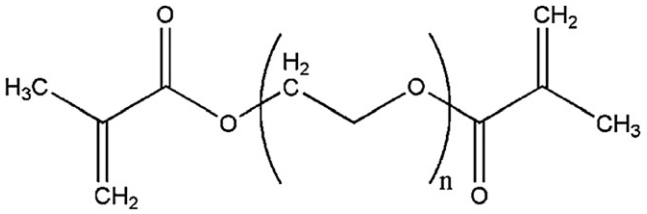

Fig. 1. Chemical structure of tri-ethylene glycol dimethacrylate ($n = 3$).

2.1. Dielectric relaxation spectroscopy

The dielectric measurements were carried out using an impedance analyzer, covering a frequency range from 10^{-1} Hz to 2 MHz. A drop of the AIBN/monomer mixture with two silica spacers 50 μm thick was placed between two gold plated electrodes (diameter 20 mm) of a parallel plate capacitor. The sample cell was mounted on a cryostat and exposed to a heated gas stream being evaporated from a liquid nitrogen Dewar. The temperature control is performed within ±0.5 °C.

To verify that all samples did not polymerize during the storage, these were monitored from room temperature to −120 °C at a cooling rate of around 8 °C min^{-1} and compared with isochronal data for the TrEGDMA pure monomer taken from reference [10].

After this cooling scan to −120 °C, the temperature of the samples was sharply increased to the final polymerization temperature, T_{pol} (62, 66, 70 or 75 °C). Dielectric loss spectra were collected isothermally at T_{pol} every 90 s, during 2.5 h for each sample. The real and imaginary parts of the complex permittivity were measured at 29 frequencies within the range from 0.7 Hz to 1 MHz, in such a way that each loss spectrum was collected in a period of time that does not exceed 1 min, trying to assure that no significant changes occur during each frequency scan.

Post-curing treatment consisted in cooling the polymerized sample to −120 °C and reheating up to 220 °C at around 10 °C min^{-1}. By this way, polymerization of the remaining monomer and probably consumption of unreacted double bonds in the polymer network was induced. After that, the sample was cooling again down to −120 °C in order to verify that no further polymerization occurs. The overall experimental protocol above described is displayed in Scheme. 1.

3. Results

3.1. Conductivity in the unreacted system

The dielectric loss spectra, ε″(f), for the TrEGDMA monomer taken from −120 to 25 °C were presented and analyzed in references [10,11]. The more important features were the detection of three dipolar relaxations: the α-relaxation related to the glass transition, and two secondary, β and γ, corresponding to more localized motions. Data were affected by high conductivity that manifested at temperatures as low as −70 °C. This effect was accounted for in the fit of the ε″ spectra by including the term $i\sigma/\omega^c\varepsilon_0$ (ε_0 is the vacuum permittivity, σ and c are fitting parameters). The contribution of dc conductivity which is undesirable when

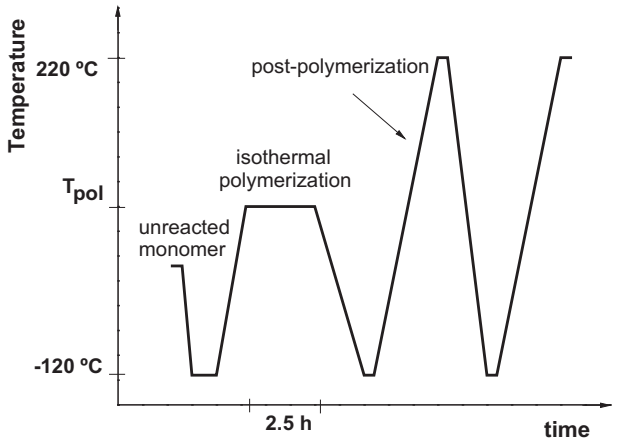

Scheme 1. Representation of the temperature/time protocol followed to monitor polymerization changes.

analyzing dipolar relaxation will allow us obtaining information about the evolution of the system during isothermal polymerization using conductivity itself and modulus formalism.

In the modulus representation, besides the peak related to segmental motions (M″(α)) there is another one associated to dc conductivity (M″(σ)). The spectrum presented in Fig. 2 illustrates these two contributions at −62 °C. As expected [12] the position of the alpha relaxation peak in M″ is shifted to higher frequencies relatively to the ε″-peak.

The model function introduced by Havriliak and Negami [12,13] can be adapted to a good approximation to fit the modulus spectra in accordance with the expression [12]:

$$M^*_{HN}(\omega) = M_\infty + \frac{\Delta M}{\left(1+\left(-i(\omega\tau_{HN-M})^{-1}\right)^{\alpha_{HN}}\right)^{\beta_{HN}}} \quad (7)$$

with $\Delta M = M_0 - M_\infty$ and α_{HN} and β_{HN} describe the symmetric and asymmetric broadening being $0 < \alpha_{HN}, \alpha_{HN}\beta_{HN} \leq 1$. Above −70 °C, it was necessary to include the peak related to conductivity in order to reproduce the overall spectra (the solid lines in Fig. 2 are the resulting fit). From the estimated values of τ_{HN}, α_{HN} and β_{HN}, a model-independent relaxation time $\tau_{max} = (2\pi f_{max})^{-1}$ was calculated according to [12]:

$$\tau_{max} = \tau_{HN}\left[\sin\left(\frac{\alpha_{HN}\pi}{2+2\beta_{HN}}\right)\right]^{-\frac{1}{\alpha_{HN}}}\left[\sin\left(\frac{\alpha_{HN}\beta_{HN}\pi}{2+2\beta_{HN}}\right)\right]^{\frac{1}{\alpha_{HN}}} \quad (8)$$

The obtained parameters are presented in Table 1 which also includes the equivalent values taken from the fit of the data expressed by ε″. The relaxation times $\tau_{M''(\alpha)}$ follow a VFT law (see open circles in Fig. 3). This temperature dependence can be compared with that obtained from the ε″ analysis (filled circles). The VFT fitting parameters describing both $\tau_{M''(\alpha)}(T)$ and $\tau_{\varepsilon''(\alpha)}(T)$ are summarized in Table 1. From the $\tau_{M''(\alpha)}(T)$ parameters, a glass transition temperature of −89.8 °C was estimated in very good agreement with the value obtained from $\tau_{\varepsilon''(\alpha)}(T)$ [10] and the calorimetric one (−86 °C) [11].

The M″-peak related to conductivity, M″(σ), (remember Fig. 2) can be well described considering the shape parameters $\alpha_{HN} = \beta_{HN} = 1$, *i.e.* a Debye peak. In this case is possible to construct a master curve indicating that the conductivity relaxation doesn't change in nature in this temperature region (from −70 to 25 °C). In what concerns the intensity of the electric modulus, $\Delta M = M_0 - M_\infty$, it is noteworthy the accentuated increase between −50 and −30 °C, followed by a suddenly drop at −20 °C, after which it returns to the trend found at temperatures lower than −50 °C (see inset in Fig. 3). This effect is possibly related to the occurrence of crystallization and subsequent melting phenomena. In fact, cold-crystallization in this temperature range was also observed for the other members of the n-ethyleneglycol dimethacrylate family such as EGDMA ($n = 1$) and TeEGDMA ($n = 4$) [14–16]. The temperature dependence of the characteristic relaxation time, $\tau_{M''(\sigma)}$, is also included in Fig. 3 (open squares) and denotes a clear departure from the Arrhenius behavior. The parameters obtained for the VFT curve fit are presented in Table 2.

However, the conductivity mechanism can be also studied directly from the conductivity analysis. The real part of the conductivity from −115 to 25 °C is presented in Fig. 4, having, at the highest temperatures, the typical profile exhibited by a variety of quite different disordered materials, *i.e.* a plateau at the lowest frequencies that bends off to a frequency dependent behavior at a critical frequency, named ω_c (crossover frequency [17]). At the lowest temperatures the real conductivity spectra comes affected by dipolar relaxation.

Using the so called 'Summerfield scaling', it was possible to construct a master curve [18] which is shown in inset of Fig. 4. Four regions are able to be distinguished in this representation: region A – where electrode polarization dominates the dielectric response due to space charge accumulation at the sample/electrode interface, that is felt at temperatures higher than −40 °C; region B – a plateau in the conductivity corresponding to frequency

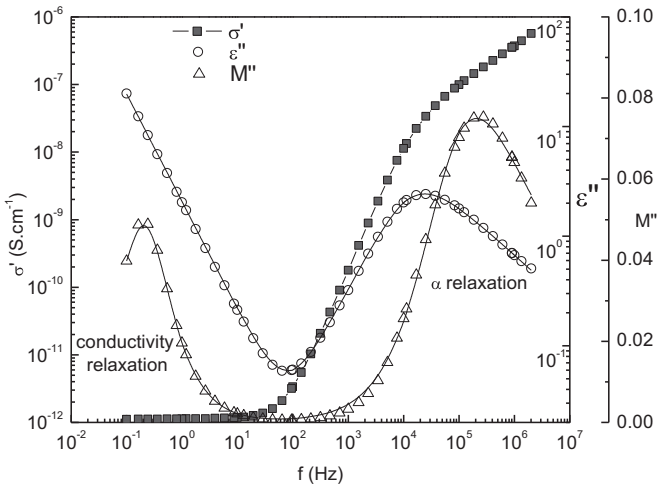

Fig. 2. Spectrum taken at −62 °C: σ′ in left axis (filled squares), and in the right axis ε″ (open triangles) and M″ (open circles). Solid lines in ε″ and M″ are the corresponding HN fitting curves.

Table 1
Shape parameters α_{HN} and β_{HN}, values of the VFT coefficients, glass transition temperature obtained considering $\tau = 10^2$ s and fragility index for the α-relaxation of bulk TrEGDMA obtained from the spectra of ε″ and M″ respectively.

	$\tau_{\varepsilon''(\alpha)}$[a]	$\tau_{M''(\alpha)}$
α_{HN}	0.95 ± 0.02	0.76 ± 0.02
β_{HN}	0.46 ± 0.02	0.40 ± 0.02
τ_0/s	(2 ± 1) × 10^{-15}	(3 ± 2) × 10^{-16}
B/K	1439 ± 8	1398 ± 44
T_0/K	147 ± 1	149 ± 2
T_g/K	185.5	183.2
m	85	97

[a] Data corresponding to α relaxation are taken from reference [10].

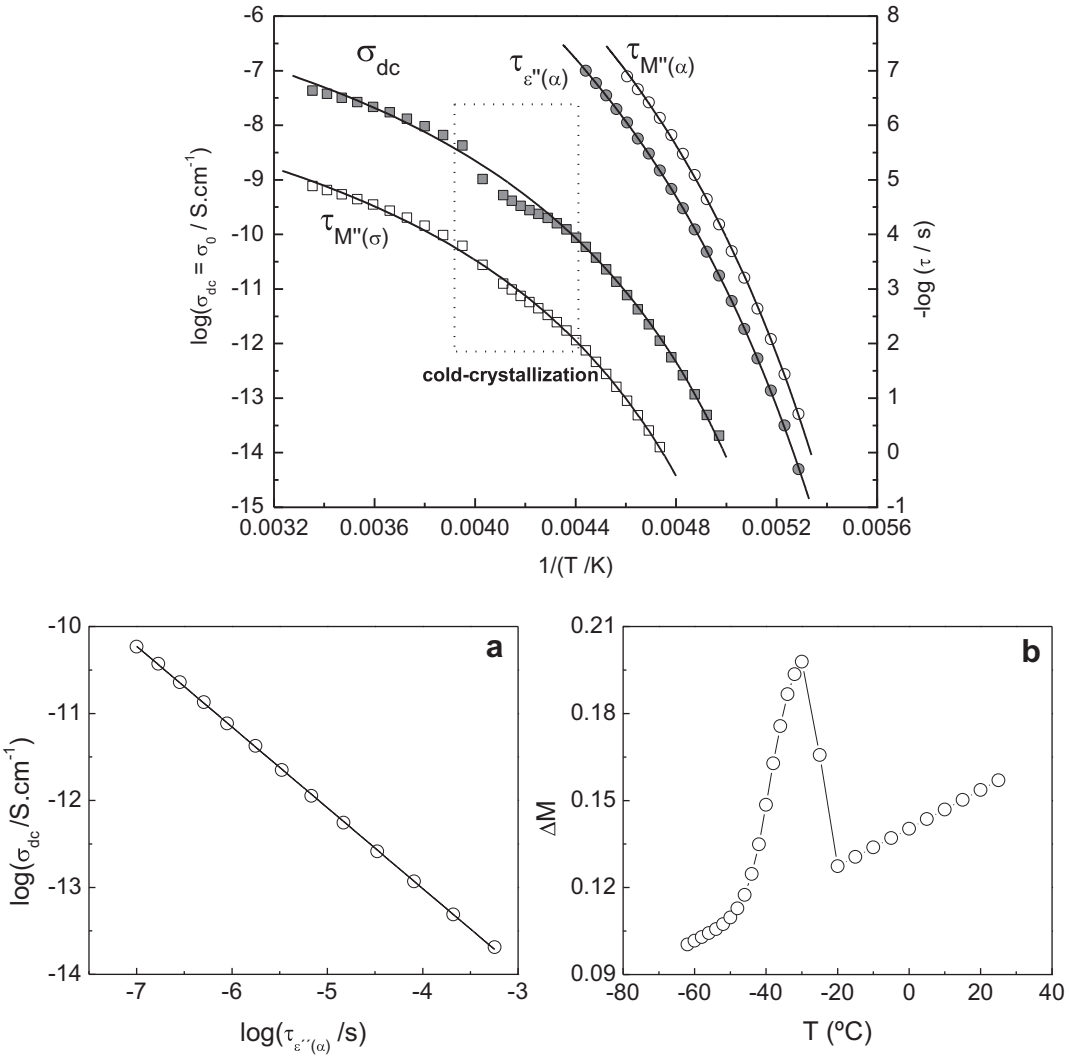

Fig. 3. Arrhenius plot for DC conductivity taken directly from the plateau in σ′ representation, filled squares, left axis. In the right axis are represented the relaxation time (τ_{max}) of: α process obtained from HN fitting of ε″, filled circles [10]; α and σ processes obtained from HN fitting of M″, with open circles and open squares respectively. The lines are the corresponding VFT curves. The dashed square indicates the temperature range where crystallization/melting occur. The insets represent the linear relation between σ_{dc} and $\tau_{\varepsilon''(\alpha)}$ in log–log scales ($r^2 = 0.9998$) proofing that the relation $\sigma.\tau^k$ = constant holds (in this particular case $k = 1$) and the temperature dependence of ΔM taking from the HN fitting of the σ-peak.

independent conductivity σ_{dc}; region C corresponds to the presence of the α-relaxation associated with dynamic glass transition confirmed by the loss peak that emerges in the same location (Fig. 2); the linear slope for region C was estimated as 0.97 ± 0.02. Finally, in region D, the usual frequency dependence behavior of conductivity (a.c. conductivity) is found, following the general power law dependence $\sigma \sim \omega^s$ (with $s \leq 1$) [17] with $s = 0.60 \pm 0.02$.

The simultaneous detection of segmental mobility and conductivity that collapse in the single master plot obtained earlier, implies identical thermal activation [19] of both glassy dynamics and charge transport processes for TrEGDMA as found for imidazole-based glass formers [20].

The value of dc conductivity (σ_{dc}) for each isotherm between −72 and 25 °C can be taken from the plateau in conductivity (region A depicted in Fig. 4) which increases with the temperature increase. Its representation in the activation plot (see filled squares in Fig. 3) clearly shows a non-Arrhenius behavior as previously found for $\tau_{M''(\sigma)}$(T). The discontinuity in the values of σ_{dc} observed at temperatures around −35 °C is due, as mentioned above, to cold-crystallization that must be occurring in such a way that conduction mechanisms are affected. Without considering

Table 2
VFT parameters obtained for the temperature dependence of the relaxation time of the modulus peak associated with conductivity ($\tau_{M''(\sigma)}$) and for dc conductivity. In any case, points affected by cold-crystallization or melting were not considered.

	$\tau_{M''(\sigma)}$	σ_{dc}	σ_{dc}[a]
	τ_0/s (5 ± 1) × 10^{-8}	σ_0/S.cm^{-1} (2.6 ± 0.6) × 10^{-5}	σ_0/S.cm^{-1} (2.6 ± 0.6) × 10^{-5}
B/K	676 ± 33	797 ± 34	C/K^{-1} = 4.85 ± 0.26
T_0/K	170 ± 2	163 ± 2	163 ± 2

[a] VFT modified in accordance with Equation 12(b) to fit σ_{dc} data.

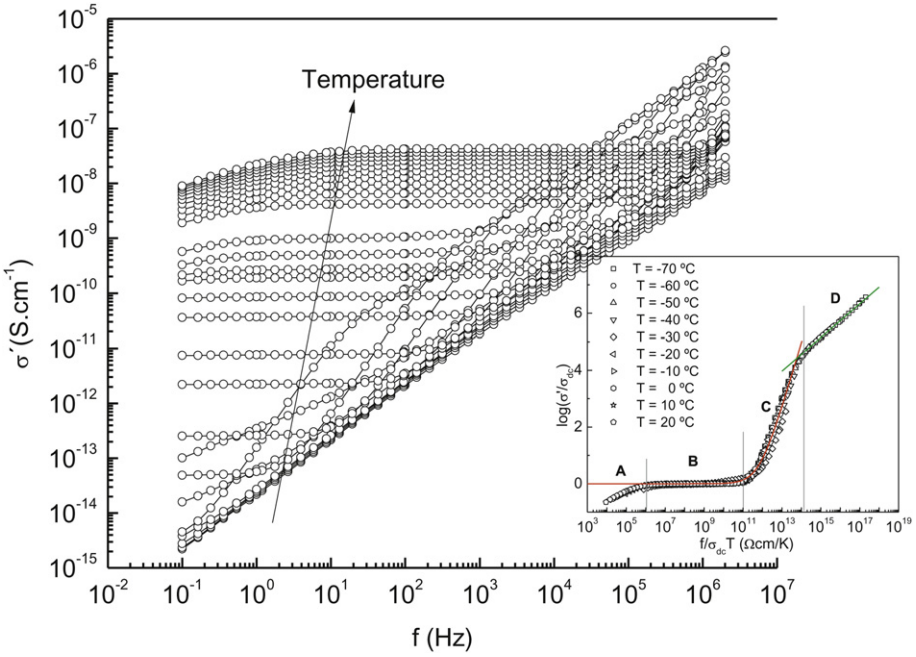

Fig. 4. Variation of the real part of the complex conductivity vs. frequency for the temperature range from −115 to 25 °C (only the isothermal data taken approximately every 5 °C are shown). Inset: Conductivity master curves for selected temperatures from −70 to 20 °C every 10 °C. The master curves were generated by using Summerfield scaling. The curvature in the high frequency side corresponds to the relaxation of dipolar origin. The red line represents the master curve with Jonscher's equation ($s = 1$) and the green line corresponds to $s = 0.59$. (For interpretation of the references to colour in this figure legend, the reader is referred to the web version of this article.)

those points in the region of crystallization/melting, a VFT function with parameters $\sigma_\infty = 10^{-4.6} = 2.5 \times 10^{-5}$ S cm^{-1}, $B = 797$ K and $T_0 = 163$ K well describes the observed curvature (Table 2). The temperature dependence of σ_{dc} could be originated by the non-Arrenhian dependence of the segmental mobility. In fact, the direct comparison of σ_{dc} and $\tau_{\varepsilon''(\alpha)}$ in log–log scale is displayed in the inset of Fig. 3, and the linear fit with r^2 of 0.9998 denotes the correlation between these two quantities (similar results were found for imidazole [20] and propylene glycol [6]).

3.2. Monitoring the reaction

Since the TrEGDMA monomer is in the liquid state at high temperatures (around 70 °C), in the range of the isothermal polymerizations studied, the dielectric spectra are characterized by a high conductivity (see open squares in Fig. 5). The data collected during the reaction present this contribution during the whole polymerization though the value of ε″ changes until reaching an equilibrium value depending on T_{pol}. In what concerns the dielectric constant ε′, it shows a plateau at high frequencies and it increases significantly in the low frequency side (filled squares in Fig. 5), precisely where the loss factor deviates from a linear tendency with slope −1 in the log–log representation. Such high values of ε′ at low frequencies may be due to the interfacial effects within the bulk of the samples and also may be partially due to the electrode effects. At the beginning, the blocking of charge carriers at the sample/electrodes interfaces is in the origin of this additional contribution, *i.e.* the electrode polarization. After polymerization, two phases coexist, unreacted monomer and polymer network, leading to the accumulation of charges at the internal phase boundaries, which results in the well-known Maxwell-Wagner-Sillars effect [21–23]. Although presenting similar features to electrode polarization, this interfacial polarization has a lower intensity [24] and turns to be the dominating effect at lower frequencies during reaction.

In any case, neither ε′ nor ε″ representations allow to extract reliable information about the progress of polymerization. Oppositely, the representation of the electric modulus allows a more detailed analysis of underlying changes since the spectra of M″ exhibits a pronounced relaxation peak which changes during the polymerization time as it can be observed in Fig. 6. In this representation, the space charge effects are suppressed and the existing peak reveals an ionic conductivity [25–27].

Equation (7) was used to fit data of M″ by fixing the $\alpha_{HN} = 1$ and the remaining parameters were allowed to vary. The β_{HN} shape parameter was found to be 0.95 ± 0.05 for all T_{pol}. The characteristic time, $\tau_{M''}$, changes upon polymerization in accordance with Fig. 7 (a), where data for the four polymerization temperatures are

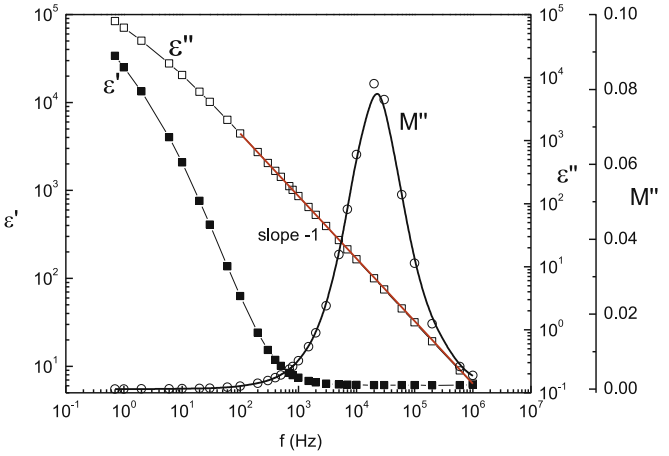

Fig. 5. Dielectric results for TrEGDMA/AIBN mixture at $T_{pol} = 66$ °C at the initial time: in left axis the real part of ε* (filled squares) and in the right axis the imaginary part of ε* (open squares) and M* (open circles); the representation of the dielectric modulus included the HN fitting.

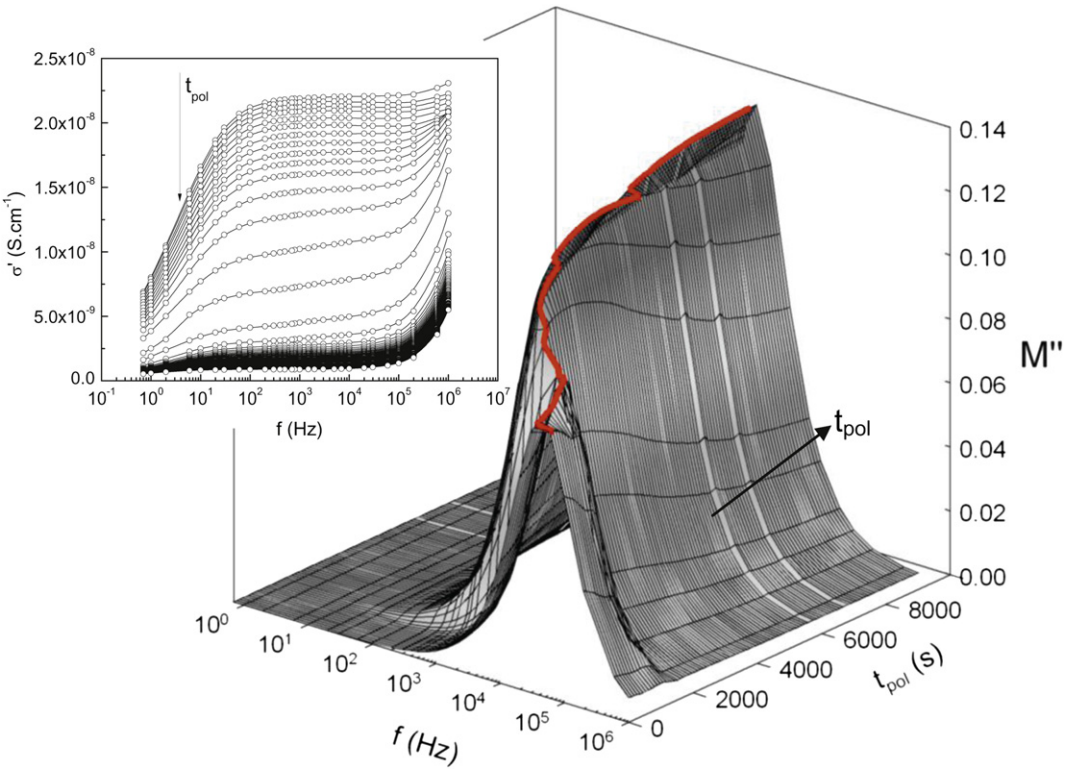

Fig. 6. 3D representation of electric modulus *vs.* frequency and polymerization time for $T_{pol} = 70\ ^{\circ}C$. The solid red line indicates the evolution of the M″- maximum with t_{pol} only for user-guide; the inset depicts the evolution of correspondent real conductivity spectra. (For interpretation of the references to colour in this figure legend, the reader is referred to the web version of this article.)

included. After an initial stage where $\tau_{M''}$ does not vary significantly with the polymerization time, t_{pol} defining more or less a plateau, a sudden increase occurs at a different time for each T_{pol}. The intensity of the M″-peak (not shown) follows the same trend undergoing also an abrupt increase at exactly the same t_{pol}.

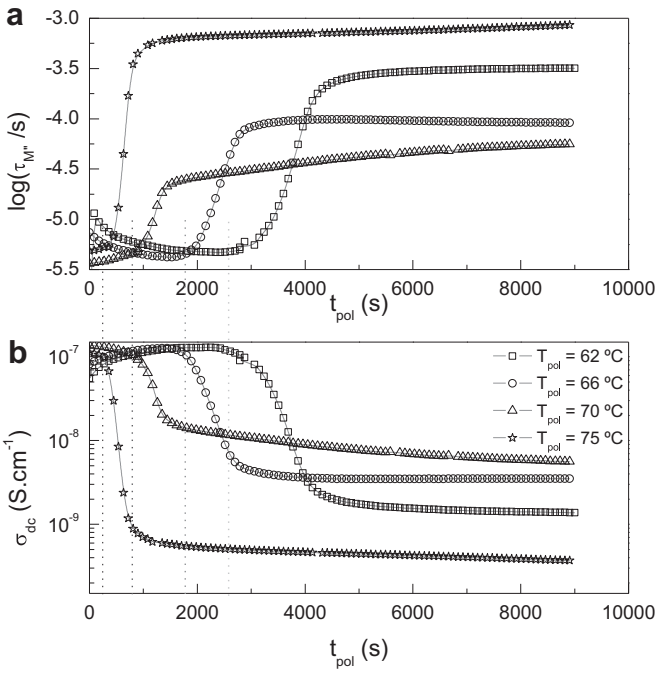

Fig. 7. a) Relaxation time, $\tau_{M''}$, taken from HN fitting and b) dc conductivity values *vs.* polymerization time.

By other side, the polymerization can be also monitored through the conductivity variation. In the inset of Fig. 6, the evolution of the real conductivity spectra with polymerization time, t_{pol}, is shown at a representative temperature ($T_{pol} = 70\ ^{\circ}C$). The plateau related to the σ_{dc} is the predominant feature observed in the spectra. The increase associated to σ_{ac} starts at frequencies (crossover frequency, ω_c) in the limit of our frequency window. On the other hand, the decrease at frequencies below 100 Hz is attributed to electrode polarization as mentioned earlier.

The conductivity decreases with the polymerization time as expected. However, the relatively high values of σ_{dc} at the end of the polymerization (the conductivity only drops two decades on average), suggests that not all the monomer has been consumed. This was confirmed in the subsequent cooling where the α process of the monomer was still detected, being higher for sample polymerized at 70 °C. Unreacted monomer is still detectable in this sample even after post-polymerization carried at 220 °C; for the other samples polymerized at different T_{pol}, no evidences of monomer were found at the end of this thermal treatment (see Fig. 8).

The drop of σ_{dc} values (taken from the plateau in σ') upon reaction, as shown in Fig. 7(b), evolve in a symmetrical way relative to the increase in $\tau_{M''}$. Vertical lines indicate the agreement between the onset time taken from conductivity and modulus which are listed in Table 3. While M″, from which $\tau_{M''}$ is obtained, contains simultaneously the contribution of ε' and ε'', *i.e.* of, capacitance and resistance, respectively, the real conductivity is only obtained from the reciprocal of the resistance of the electrical equivalent circuit being a more direct property. For that reason, the agreement between the evolution of these two quantities, σ_{dc} and $\tau_{M''}$, validates the use of the latter to follow the polymerization kinetics. An additional advantage of using the dielectric modulus is to obtain in a straightforward manner the mobility of charge carriers by its relaxation time.

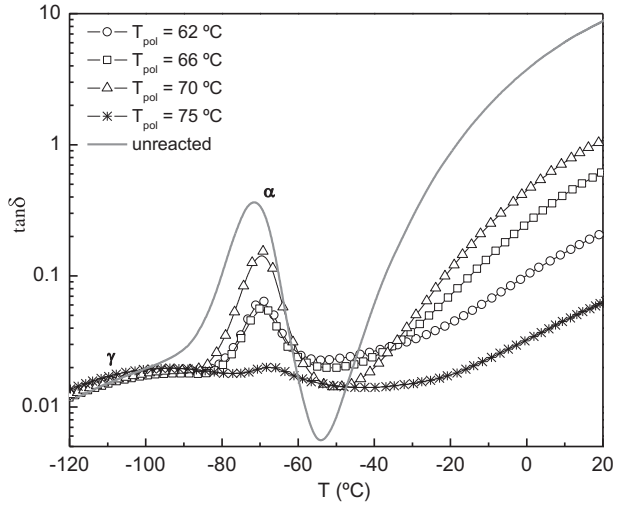

Fig. 8. Temperature dependence of tanδ at 1 kHz obtained after isothermal polymerization at the temperatures indicated inside. Data were collected at a cooling rate of around 9 °C min^{-1}. The solid gray line was taken from reference [10] corresponding to the bulk monomer.

Under these particular conditions of polymerization reaction, neither the modulus nor conductivity is affected by any segmental motion contribution. In this case, oppositely to what happened in the unreacted system, it is possible to use σ_{dc} and/or $\tau_{M''}$, to extract information about charge transport.

The charge transport mechanism is described as the hopping of charge carriers in a random spatially varying potential landscape; unlike crystals, the potential-energy landscape experienced by an ion in a disordered solid is irregular and contains a distribution of depths and barrier heights (schematic representation in ref. [28]). Basically the transport process, as proposed by Dyre, is governed by the ability of charge carriers to overcome the randomly distributed barriers. On short time scales only the smallest barriers are surmounted and the dynamics is characterized by back-and-forth motion over limited ranges: "sub-diffusive" regime. As time passes, higher and higher barriers are surmounted, and eventually the highest barriers are overcome achieving an infinite cluster of hopping sites, resulting in long-range ion transport that determines the onset of dc conductivity, *i.e.* of a "diffusive" dynamics of charge transport. The frequency that defines the transition form a sub-diffusive to a diffusive regime is designated crossover frequency (ω_c) that is taken as a measure of the attempt rate, ω_e ($=1/\tau_e$), of the charge carriers to overcame the highest energy barrier. The empirical form for the real conductivity, $\sigma'(\omega)$, is given by a power law dependence on frequency as proposed by Jonscher [29],

$$\sigma'(\omega) = \sigma_{dc}\left[1 + \left(\frac{\omega}{\omega_c}\right)^s\right] \quad (9)$$

where 's' ($0.5 \leq s \leq 1$) [17] is a material and temperature dependent parameter, allowing to obtain ω_c. This parameter, ω_c, has been taken to extract reliable values of diffusion coefficients of migrating charges, D, by using the Einstein relation that reads:

$$D = \frac{\lambda^2}{2\tau_h} \quad (10)$$

where λ is the hopping length (comparable to the Pauling diameter *i.e.* 0.2 nm, with negligible temperature dependence [30,31],) and τ_h, the hopping time. The general equation for the diffusion coefficient equals D to $< r^2 > /2.d.\tau_h$, where $< r^2 >$ is the mean-square distance that a particle can jump when diffusing in a time τ_h and *d* the number of dimensions of the particle movement; Equation 10 assumes a one-dimensional motion ($d = 1$) as compatible with the dielectric experimental setup where parallel plate capacitor configuration is used. By setting $\tau_h \cong 1/\omega_c$ [31] it is possible to extract the value of the diffusion coefficients from which the mobility is readily determined.

In the present study, it seems useful to compare the diffusion coefficients of charge carriers at the end of each isothermal polymerization. This allows obtaining some qualitative information about the network structure. The parameters obtained from the fitting of experimental data with Fig. 9 and the estimated diffusion coefficients are presented in Table 3.

Table 3
Average time taken of the inflexion of the sigmoidal variation of the relaxation time (extracted from the position of the M″-peak) and the dc conductivity (see vertical lines in Fig. 7); relaxation time of M″-peak at the end of isothermal polymerizations; parameters obtained by fitting with Jonscher's equation at the end of isothermal polymerizations and diffusion coefficients estimated from equation (9) considering ω_c.

T_{pol} (°C)	$\tau_{M''}$		Jonscher			D ($cm^2.s^{-1}$)
	t_{onset} (s)	$\tau_{M''}$ end-polymerization	σ_0 ($S.cm^{-1}$)	ω_c (rad)	s	
62	2560 ± 60	3.2×10^{-4}	1.3×10^{-9}	1.3×10^{5}	0.96	2.5×10^{-11}
66	1750 ± 60	9.1×10^{-5}	3.5×10^{-9}	5.8×10^{5}	1.00	1.2×10^{-10}
70	765 ± 60	5.6×10^{-5}	5.4×10^{-9}	1.1×10^{6}	0.97	2.2×10^{-10}
75	200 ± 70	8.6×10^{-4}	3.5×10^{-10}	8.3×10^{4}	1.01	1.7×10^{-11}

4. Discussion

TrEGDMA is a glass former with a glass transition temperature of −86 °C as determined by differential scanning calorimetry [11]. Thanks to this low value of T_g, a large temperature range is available for studying the conductivity in the supercooled and liquid state. With this aim, σ′ as well as M″ were the physical properties analyzed in depth.

Using the modulus representation, a well defined peak associated to conductivity is already detected in isothermal spectra near and above −70 °C (remember Fig. 2). The fitting of these spectra considering the HN function reveals that the shape parameters α_{HN} and β_{HN} are equal to 1. In accordance with Sheoran [32] a Debye

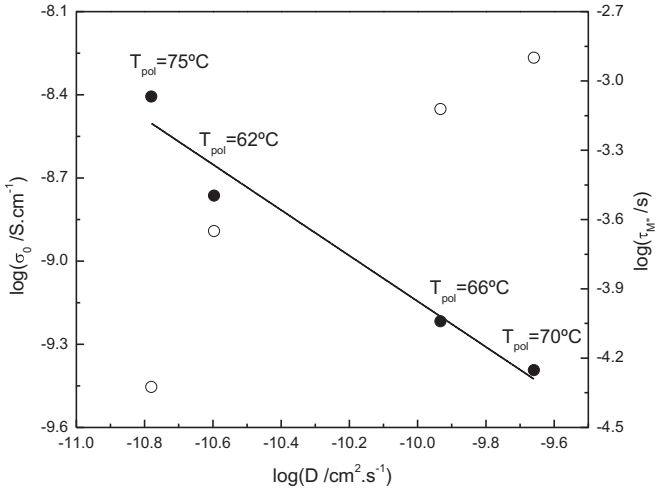

Fig. 9. DC conductivity in left axis and filled symbols, and relaxation time of M″ in right axis and open symbols *vs.* the diffusion coefficients obtained at the end of the isothermal polymerizations.

behavior is exhibited by an ideal dielectric or a glass having very low concentration of mobile ions. Moreover, these shape parameters remain constant in the temperature range available, allowing us to construct a master curve. Also the analysis of the conductivity, σ′, supports this constancy in the shape spectra, indicating that the conduction mechanisms are not affected by temperature changes.

In what concerns the temperature dependence of the relaxation times and d.c. conductivity extracted from the spectra, the undoubtedly departure of the Arrhenius behavior of both properties is noteworthy. This curvature is well fitted by using the VFT equation and in the activation plot (Fig. 3) $\log(\sigma_{dc})$ and $\log(\tau_{M''(\sigma)})$ evolve in parallel (note that B and T_0 taken from VFT fitting functions (Table 2) are very similar). This fact suggests a relation between σ′ and M″ confirmed by the linearity of the representation of $\log(\tau_{M''(\sigma)})$ versus $\log(\sigma_{dc})$ (r^2 higher than 0.99).

At this time it seems convenient to pay attention also to the VFT behavior followed by the α process associated to the dynamic glass transition (well seen by either M″(α) or ε″ spectra). This temperature dependence of the dipolar relaxation close to T_g, or in other words, the fragile character of TrEGDMA, is probably in the origin of the temperature dependence of the conductivity which probes a translational diffusion mechanism of the charge carriers. In fact the log–log representation of σ_{dc} *vs.* τ_α gives a straight line (remember inset in Fig. 3) suggesting a correlation between translational motions and reorientational mobility described by $\sigma\tau^k =$ constant as found for others glass formers [33,34]. To test this, the 'decoupling index', $R\tau(T_g)$, was determined for each material which is the ratio of the structural relaxation time to the conductivity relaxation time, giving a physical idea of the relation between the conductivity and structural relaxation processes. This factor conveniently describes the extent to which the ion conducting motions in a given glass can be considered decoupled from the viscous motions of the glassy matrix. An approximate relation between the logarithm of the decoupling index and the conductivity (in S cm^{-1}) measured at T_g was proposed by Angell [35]:

$$\log(R_\tau(T_g)) = 14.3 + \log(\sigma_{dc}(T_g)) \tag{11}$$

giving the orders of magnitude of the mobility of the charge carriers relative to the mobility driven by the segmental dynamics. The σ_{dc} value obtained at the dielectric T_g, is 2.10^{-16} S cm^{-1} giving a decoupling index of 0.04 (for imidazole the value found was close to 2 [20]). The low value estimated confirms the correlation between the dynamics of the segmental relaxation and the ion motion.

Since in the TrEGDMA monomer both glass transition temperature and conductivity are well determined, it is possible to test the relation proposed by Angell [35,36]:

$$T_g = T_0'(1 + 0.0255C) \tag{12a}$$

$$\sigma_{dc} = \sigma_0 \exp\left(-\frac{CT_0'}{T - T_0'}\right) \tag{12b}$$

where C and T_0' are obtained from the temperature dependence of conductivity as described by a modified VFT equation [35]; the C notation was adopted instead of the usual D to avoid confusion with the diffusion coefficient.

The estimated fitting parameters obtained with Equation 12(b) are included in Table 2, predicting a glass transition temperature, according Equation 12(a), of 183.3 K (−89.9 °C) in excellent agreement with both calorimetric and dielectric T_g values and therefore providing a further evidence of the validity of that equation. In systems for which the temperature dependence of the segmental motions is not unequivocally detectable due to the superposition of conductivity, it is useful to have this kind of relations in order to determine the dielectric T_g. With this aim, Leys and co-workers [37] have used an ad hoc value of $\sigma(T_g) = 10^{-14}$ S cm^{-1} (10^{-12} S m^{-1}) to extract a glass transition temperature from the conductivity data. Clearly this criterion is not fulfilled by TrEGDMA since both at the calorimetric T_g (−86 °C) or at the temperature at which the relaxation time of main dipolar relaxation is 100 s (−89.9 °C) the value of conductivity is in the order of 10^{-16} S cm^{-1}, *i.e.* two orders of magnitude below the value proposed by Leys. This discrepancy in σ (T_g) values, possibly related to a different origin of conductivity, suggests that the tentative of establishing a universal constant value of conductivity to define T_g is not straightforward (for several polymeric materials under investigation in our group we verify that the conductivity at T_g is always around 10^{-15}-10^{-16} S cm^{-1}).

Contrary to what happens while probing the monomer mobility at temperatures in the range or below its glass transition where both orientational and charge transport contribute to the dielectric response, during polymerization the latter is the dominant contribution. Therefore in the modulus representation at T_{pol}, where the unreacted monomer is in the liquid state, only the peak associated with conductivity (M″(σ)) appears. This peak will be taken now for further investigation together with the real conductivity, σ′.

From the analysis of the evolution of the relaxation time obtained from the fit of the modulus peak ($\tau_{M''(\sigma)}$) with polymerization time (t_{pol}), two principal aspects must be pointed out (remember Fig. 7(a)): *i*) this parameter experiments a sudden increase at a certain polymerization time t_{pol}, taking place sooner as the polymerization temperature increases; *ii*) the $\tau_{M''(\sigma)}$ of the final network increases with increasing the polymerization temperature from 62 to 70 °C, but it decreases for the highest temperature *i.e.* 75 °C.

In order to understand the meaning of these changes it is convenient to remember a previous study of the isothermal polymerization of TrEGDMA/AIBN carried out by using temperature modulated differential scanning calorimetry (TMDSC) [9]. It was reported that the sudden drop detected in the heat capacity measured during isothermal polymerization was due to the vitrification of the growing polymer network, corresponding the faster reaction onset to the higher T_{pol}. In a similar way, the abrupt change in the relaxation time taken from the analysis of electric modulus can be related to this phenomenon. Vitrification can be rationalized considering that during glass transition the conformational rearrangements of the polymer chains becomes frozen and this hinders the motion of space charges. Thus, at the same time that the heat capacity of the sample drops, the relaxation time of the ionic carriers displacement sharply increases and the conductivity decreases. However, although sharp, the step in both conductivity and $\tau_{M''}$ is relatively small. To explain this, it is convenient again to take in mind another important result obtained from TMDSC analysis [9], which consists in the phase separation that takes place between the unreacted monomer and the polymer under formation. Vitrification is expected to happen at a conversion for which the glass transition temperature of the mixture of the growing network and the remaining monomer equals polymerization temperature, but as a consequence of phase separation, the reaction stops when the monomer content is much higher than expected for a homogeneous mixture. In fact, a further evidence of phase separation was already mentioned in the previous section when it was detected the interfacial polarization (at advanced stages of polymerization). By this way, we can assume that the mobility of the remaining monomer is the main factor that determines the conductivity contribution. Such assumption leads to two important conclusions: *i*) the reaction must stop after vitrification as it is manifested by the plateau

attained for each T_{pol} (remember Fig. 7(a)), and *ii*) the possible existence of a relatively high content of the unreacted monomer will be reflected in the high values of σ' and $\tau_{M''}$ reached after vitrification as it was found. The latter was confirmed by the detection of the α-peak associated to the segmental motions of bulk TrEGDMA after isothermal polymerization (Fig. 9). In the case of isothermal polymerization of TeEGDMA ($n = 4$) under similar experimental conditions, the final relaxation time ($\tau_{M''(\sigma)}$) is much slower reaching values around 10^{-2} s and no signal of alpha-peak is detected after polymerization [38].

As shown in Fig. 7, the polymerization time at which vitrification takes place decreases with increasing temperature as expected and in good agreement with TMDSC experiments [9]. It was shown by TMDSC that the amount of remaining monomer that acts as solvent at the vitrification time, decreases with increasing polymerization temperature. Interestingly, in the T_{pol} interval between 62 and 70 °C higher temperatures yield smaller values of the relaxation time and higher value of dc conductivity attained at long polymerization times. Assuming that $\tau_{M''(\sigma)}$ is characteristic of the mobility of the remaining monomer forming a liquid phase distributed in small domains separated from the polymer, this temperature dependence is qualitatively as expected: an increase of temperature increases mobility of the bulk monomer as was shown in Fig. 4. Nevertheless, the difference of around one decade in time between 62 and 70 °C is larger than what can be estimated by extrapolation of the activation plot of Fig. 4. Thus, the microstructure of the formed network must play a role as well in the mobility of charge carriers. When polymerization is performed at 75 °C the behavior changes and the values of the relaxation time and dc conductivity shows that the monomeric mobility is much restricted than at lower temperatures. It was shown in our precedent study [9] that the sample polymerized at 75 °C is the one for which the glass transition temperature is closer to the value predicted by the Fox equation and therefore it is nearly an homogenous mixture. Thus, if phase separation does not take place, the remaining monomer is enclosed in the glassy polymer `phase and its contribution to charge transport is very restricted.

Another interesting point is the presence of monomer in the sample even after different post-curing treatments. The presence of the main dipolar relaxation of the monomer is a clear prove of the existence of a liquid monomer phase. This effect is especially clear in the sample polymerized at 70 °C in which no complete consumption of monomer was attained even after heating up to 220 °C. The explanation of this phenomenon can be found in the lack of initiator molecules in the liquid phase once phase separation takes place. Probably in this case, the microstructure obtained after isothermal polymerization consists in a dense crosslinked network that expels out the unreacted monomer, the latter persisting into (or forming) large domains giving rise to a bulk-like dielectric response. The coexistence of monomer pools and highly crosslinked regions is usually observed as a result of the formation of microgel regions upon free radical polymerization of multifunctional monomers [39] as TrEGDMA. Indeed, when the monomers are multifunctional, primary cyclization occurs between pendent double bonds and radicals, contributing to microgel formation and hence to heterogeneity.

On the other hand, in order to compare the final networks obtained for each T_{pol}, we can calculate the diffusion coefficients. The fitting of $\sigma'(\omega)$ data taken at the end of each isothermal polymerizations, provides the crossover frequency which is useful to estimate the hopping time necessary to introduce in Equation 10. As shown in Fig. 9, the diffusion coefficients in the final polymers seem to be correlated with relaxation time, $\tau_{M''(\sigma)}$ (in log–log representation, $r^2 > 0.94$), rather than with the dc conductivity ($r^2 = 0.85$). This is an important point since being so, it is confirmed that $\tau_{M''}$ and D refer mainly to the transport rate of charge carriers ($\log(\tau_{M''})$ being inversely proportional) while σ_{dc} is determined from both number of charge carriers and their mobility.

5. Conclusions

In the present work the behavior of TrEGDMA both in bulk state and upon polymerization was analyzed in terms of conductivity (σ') and electric modulus (M''). In bulk TrEGDMA the modulus representation evidence two peaks related with dipolar ($M''(\alpha)$) and conductivity ($M''(\sigma)$) mechanisms. The $\tau_{M''(\sigma)}$ and the dc conductivity exhibit VFT temperature dependence, and therefore a correlation was established with the segmental mobility and the charge transport mechanism.

The mechanisms of conductivity do not change in the temperature range studied allowing the construction of a master curve for both σ' and M'' representations. In the former, besides the expected plateau of σ_{dc}, two different regimes are found: one described using the Jonscher's law with an exponent close to unity while the other, located at the highest frequencies, is described by a value of 0.60 ± 0.02. The intermediate regime is due to the influence of the intense dipolar relaxation.

The isothermal polymerization of TrEGDMA/AIBN was studied and analyzed by using the electric modulus formalism. Upon isothermal polymerization at temperatures between 62 and 75 °C, where the dipolar contribution is meaningless, the vitrification of the samples has being identified by a significant increase in the intensity and in the relaxation time of the $M''\sigma$-peak; the magnitude of σ_{dc} undergoes a sharp decrease at the same polymerization time. From the fit of the σ' curves measured at the end of polymerization, the crossover frequency was obtained and the diffusion coefficients of charge carriers in the formed network were extracted.

A correlation was proposed between transport properties exhibited after polymerization and the morphology of the formed polymer network.

Acknowledgments

Fundação para a Ciência e Tecnologia by financial support, SFRH/BPD/3961/2007.

References

[1] Wasylyshyn DA, Johari GP, Tombari E, Salvetti G. Chem Phys 1997;223:313–22.
[2] Johari GP, Ferrari C, Salvetti G, Tombari E. Phys Chem Chem Phys 1999;1:2997–3005.
[3] Venkateshan K, Johari GP. J Chem Phys 2006;125:014907(1–7).
[4] Tombari E, Ferrari C, Salvetti G, Johari GP. J Phys Conden Matt 1997;9:7017–38.
[5] Williams G, Smith IK, Holmes PA, Varma S. J Phys Conden Matt 1999;11:57–74.
[6] Pathmanathan K, Johari GP. J Chem Phys 1991;95:5990–8.
[7] Macedo PB, Moynihan CT, Bose R. Phys Chem Glass 1972;13:171–9.
[8] Provenza V, Macedo PB, Volterra V, Boesch LP, Moynihan CT. J Amer Cer Soc 1972;55:492.
[9] Viciosa MT, Hoyo JQ, Dionísio M, Gómez Ribelles JL. J Therm Anal. Calor 2007;90:407–14.
[10] Viciosa MT, Rodrigues CM, Dionísio M. J Non-Crystal Solids 2005;351:14–22.
[11] Viciosa MT, Dionísio M. J Non-Crystal Solids 2004;341:60–7.
[12] Schonhals A, Kremer F. Analysis of dielectric spectra. In: Kremer F, Schonhals A, editors. Broadband dielectric spectroscopy. Berlin: Springer-Verlag; 2003. p. 59–98.
[13] Havriliak S, Negami S. Polymer 1967;8:161–210.
[14] Viciosa MT, Correia NT, Sánchez Salmerón M, Gómez Ribelles JL, Dionísio M. J Phys Chem B 2009;113:14196–208.
[15] Viciosa MT, Correia NT, Sánchez Salmerón M, Carvalho AL, Romão MJ, Gómez Ribelles JL, et al. J Phys Chem B 2009;113:14209–17.
[16] Viciosa MT, Brás AR, Gómez Ribelles JL, Dionísio M. Eur Pol J 2008; 44:155–70.

[17] Kremer F, Rozanski SA. Analysis of dielectric spectra. In: Kremer F, Schonhals A, editors. Broadband dielectric spectroscopy. Berlin: Springer-Verlag; 2003. p. 475–93.
[18] Summerfield S. Philos Mag B-Phys Conden Mat Stat Mech Electr Opt Magn Prop 1985;52:9–22.
[19] Dyre JC, Schroder TB. Rev Mod Phys 2000;72:873–92.
[20] Iacob C, Sangoro JR, Serghei A, Naumov S, Korth Y, Karger J, et al. J Chem Phys 2008;129. 234511(1–5).
[21] Maxwell JC. Treatise on Electricity and Magnetism. New York: Dover reprint; 1892.
[22] Wagner KW. Electrical Eng (Archiv Elektrotechnik) 1914;2:371–87.
[23] Sillars RW. J Inst Electr Eng 1937;80:378–94.
[24] Steeman PAM, van Turnhout J. Analysis of dielectric spectra. In: Kremer F, Schonhals A, editors. Broadband dielectric spectroscopy. Berlin: Springer-Verlag; 2003. p. 495–522.
[25] Starkweather HW, Avakian P. J Polym Sci Part B-Pol Phys 1992;30:637–41.
[26] Tsangaris GM, Psarras GC, Kouloumbi N. J Mater Sci 1998;33:2027–37.
[27] Pissis P, Kyritsis A. Solid State Ionics 1997;97:105–13.
[28] Dyre JC, Maass P, Roling B, Sidebottom DL. Rep Progr Phys 2009;72. 046501(1–15).
[29] Jonscher AK. Nature 1977;267:673–9.
[30] Sangoro JR, Serghei A, Naumov S, Galvosas P, Karger J, Wespe C, et al. Phys Rev E 2008;77. 051202(1–4).
[31] Sangoro JR, Iacob C, Serghei A, Naumov S, Galvosas P, Karger J, et al. J Chem Phys 2008;128. 214509(1–5).
[32] Sheoran A, Sanghi S, Rani S, Agarwal A, Seth VP. J Alloys Comp 2009;475:804–9.
[33] Corezzi S, Campani E, Rolla PA, Capaccioli S, Fioretto D. J Chem Phys 1999;111:9343–51.
[34] Ediger MD. Ann Rev Phys Chem 2000;51:99–128.
[35] Angell CA. Ann Rev Phys Chem 1992;43:693–717.
[36] Angell CA. J Non-Crystal Solids 1991;131-133:13–31.
[37] Leys J, Wubbenhorst M, Menon CP, Rajesh R, Thoen J, Glorieux C, et al. J Chem Phys 2008;128. 064509(1–7).
[38] Viciosa MT, Dionísio M, Gómez Ribelles JL. Monitoring changes during network formation by dielectric measurements, In: The 6th Conference on Broadband Dielectric Spectroscopy and its Applications 2010: P-87.
[39] Lovell LG, Berchtold KA, Elliot JE, Lu H, Bowman CN. Pol Adv Mater 2001;12:335–45.